View metadata, citation and similar papers at core.ac.uk

brought to you by CORE

provided by UNT Digital Library

LAWRENCE
LIVERMORE
NATIONAL
LABORATORY

UCRL-CONF-221177

Application of imaging plate to x-ray imaging and spectroscopy in laser plasma experiments

N. Izumi, R. Snavely, G. Gregori, J. A. Koch, H-S. Park, B. A. Remington

May 7, 2006

High Temperature Plasma Diagnostics
Williamsburg, VA, United States
May 7, 2006 through May 11, 2006

Disclaimer

This document was prepared as an account of work sponsored by an agency of the United States Government. Neither the United States Government nor the University of California nor any of their employees, makes any warranty, express or implied, or assumes any legal liability or responsibility for the accuracy, completeness, or usefulness of any information, apparatus, product, or process disclosed, or represents that its use would not infringe privately owned rights. Reference herein to any specific commercial product, process, or service by trade name, trademark, manufacturer, or otherwise, does not necessarily constitute or imply its endorsement, recommendation, or favoring by the United States Government or the University of California. The views and opinions of authors expressed herein do not necessarily state or reflect those of the United States Government or the University of California, and shall not be used for advertising or product endorsement purposes.

Application of imaging plate to x-ray imaging and spectroscopy in laser plasma experiments

N. Izumi, R. Snavely, G. Gregori, J. A. Koch, H-S. Park, B. A. Remington,

University of California, Lawrence Livermore National Laboratory

P.O. Box 808, L-481, Livermore CA, 94550 USA

We report recent progress of x-ray diagnostic techniques in laser plasma experiment with using imaging plates. Imaging plate is a photo-stimulable phosphor screen (BaF(Br0.85,I0.15) :Eu^{2+}) deposited on flexible metal or plastic substrate. We applied the imaging plate to x-ray microscopy in laser fusion experiments. Self-emission x-ray images of imploded core were obtained successfully with using imaging plate and high magnification target mounted pinhole arrays. The imaging plates were applied also in ultra-intense laser experiment at the Rutherford Appleton Laboratory. Small samarium foil was irradiated by high intensity laser pulse from the Vulcan laser system. The k shell x-rays from the foil (~40keV) was used as a line x-ray source for microscopic radiography. Performance of imaging plate on high-energy x-ray backlit radiography was demonstrated by imaging sinusoidal grooves of 6um amplitude on a Au foil. Detailed spectrum of k shell x-ray from Cu embedded foil target was successfully observed by coupling imaging plate with a highly ordered pyrolytic graphite crystal spectrometer. The performances of the imaging plates evaluated in actual laser plasma experiments will be presented.

I. Introduction

Imaging plate (IP) technology was developed by early 1980's and has been used practically in medical, dental and physics experiments (J. A. Rowlands, Phys. Med. Biol. 47 (2002), Y. Amemiya, Nature 1988). At the beginning, IP technology was used as a substitute of x-ray films. Then it is found that the IP technology is applicable to various ionizing radiations and has been used in variety of applications such as electron microscopy, x-ray diffractometry, and thermal neutron imaging.

In laser plasma experiment, this technology was introduced as a detector for electron spectrometers (TANAKA POP2000, Tanaka RSI2004) and then detector for x-ray imaging (Fujioka2003, Gales2004). Compare to its rapid popularization in medical, dental and x-ray diffractometry, application of IP technology in laser plasma experiment was limited. However, it is found that the IP technology can play unique role especially in harsh electro-magnetic pulse (EMP) environment of ultra high intensity laser plasma experiments. To avoid temporal and permanent malfunction, solid-state detectors based on electric readout and their controller system has to be shielded against strong EMP from high-intensity laser plasma interactions. In contrast, IP's are totally immune to EMP interferences.

IP is a phosphor which has image storage capability. Typical IP consists of 4 layers: protection layer (plastic thickness 3~10μm); photo-stimulable phosphor layer (50~180um); polyester support layer; and metal or plastic substrate. The photo-stimulable phosphor layer is BaF(Br0.85,I0.15): Eu^{2+} crystal mixed with organic reign as binder.

Ionizing radiation absorbed in the sensitive layer excites hole-electron pairs in the crystalline phosphor. Finite fraction of those holes and electrons recombine immediately and cause scintillation like other conventional phosphors. The other fractions of them are trapped by stable electron and hole trapping center in the crystal (Takahashi, Iwabuchi). By scanning the plate with red He-Ne laser light (632.8nm), those trapped carries can be excited. Re-combination of those carriers can be read out as emission of blue light (~390nm). The spatial distribution of absorbed ionizing radiation is read out with using a He-Ne laser scanner.

Due to high Z composition of the sensitive layer, IP has good x-ray sensitivity up to 60keV. Its large dynamic range (more than 5 orders of magnitude) is also attractive for high contrast x-ray imaging, spectroscopy, and diffractometry. This rugged and relatively inexpensive detector allows its use in harsh debris environment.

Many commercially available IP scanners have capability to scan plural plates simultaneously. This gives us great flexibility in diagnostic setup of actual laser plasma experiments. One can field many imaging plates on plural lines of sight for various diagnostics without preparing cables or computers for readout. The plates can be simply wrapped light tight bag and placed wherever it is needed. This flexibility help us a lot especially during alignment test of x-ray optics like a Bragg mirrors or bent crystal imagers.

II. Performance test of imaging plate

Various kinds of IP's are commercially available. From a point of x-ray detection, most important differences of those plates are existence of protective layer and thickness and color of the sensitive layer. We tested performance of plates which is equivalent to Fuji FDL-UR-V (pigmented in deep blue), BAS-TR (intermediate blue), BAS-SR (light blue), and BAS-MS (no pigmentation). Those plates are exposed to x-ray from radioisotope standard source ^{55}Fe and ^{109}Cd and scanned by DITABIS micron scanner owned by ElectroImage, Inc.

The spatial resolution of imaging plate is limited by two factors: (1) intrinsic spatial resolution limit determined by energy transport of ionizing radiation in the sensitive layer (scattering of energetic electrons, lateral diffusion due to fluorescence of high Z material), (2) resolution limit due to optical scanning of the plate (image blur due to laser light scattered in the sensitive region and stimulate color centers in adjacent volume). For low energy x-ray, the latter is dominant. In order to increase the spatial resolution, plates optimized for high spatial resolution (e.g. FDL-UR-V) are pigmented in blue so that laser light is absorbed near the focal spot. Pigmentation of the phosphor also affects the effective depth of the sensitive layer. Due to enhanced laser light absorption in the sensitive layer, pigmented IP has highest readout efficiency on shallower surface. Then effective thickness of the plate can be thinner than its physical thickness.

a. Spatial resolution

Spatial resolutions of several different plates were tested by using calibrated radioisotope x-ray sources and a resolution test target. Fig. 1 shows the result obtained with the experiment. Image on left (right) was exposed to 5.9keV (22 keV) x-ray from ^{55}Fe (^{109}Cd) source. The test pattern is made of 20um thick gold and has binary slit pattern from 5 -20 line pair per mm. The obtained contrast transfer function was converted to the modulation transfer function (MTF) by numerically fitting the observed intensity profile (P. Pavan et al NIM 1993).

Fig.2 (a) shows MTF of various plates measured on this experiment. This result does not guarantee the performance of specific commercial products because parameter settings of the scanner (the laser focal conditions and the scan speed) were not optimized for each specific plate. As expected, the most deeply pigmented plate (FDL-UR-V) showed the best spatial resolution. The MTF for 5.9 keV x-ray was better than that of 22 keV over 10 cycle/mm region. This is explained by spectral dependence of x-ray absorption length in the sensitive layer. X-ray attenuation length in sensitive layer is estimated to be ~11um for 5.9 keV and ~204um for 22 keV. Due to scattering in sensitive layer, H-Ne laser spot is spared in the deep region. Resolution of plates with different pigmentation (BAS-TR, BAS-SR, BAS-MS) can also explained by light scattering in the sensitive layer. The deeper the pigmentation, the better spatial resolution becomes.

b. spectral sensitivity

Ignoring x-ray fluorescent from support layer, x-ray absorption efficiency in sensitive layer of IP can be estimated by,

$$h_{abs}(E) = \exp\left(-\sum_i t_i\right)\left(1 - \exp\left(-\sum_s t_s\right)\right) \qquad (1)$$

where Σ_i (Σ_s) is total x-ray cross section , t_i (t_s) is thickness of insensitive protection layer (effective thickness of sensitive layer). Assuming that all fluorescence x-ray and auger electrons are trapped and excite hole-electron pairs in the sensitive layer, spectral sensitivity is given by,

$$S(E) = E \cdot h_{abs}(E) \cdot \mu(E) \qquad (2)$$

Fig. 2 (b) shows the calculated spectral sensitivity of plate which has effective thickness of 110, 50, and 30 μm. All curves are normalized by the sensitivity for 5.9 keV x-ray. Imposed points are showing measure relative sensitivity of FDL-UR-V which has nominal phosphor thickness of 110 μm. The measured sensitivity ratio for 22 keV to 5.9 keV x-ray was 2.3 and it showed good agreement with calculated sensitivity of 110 μm thickness phosphor. Because the plate was pigmented in blue and He-Ne laser absorbed in the sensitive layer, the effective thickness of the sensitive layer expected to be thinner than its physical thickness. This in consistency could be explained by incompleteness of model (e.g. no fluorescence from supporting layer, no laser reflection from support layer). This issue (effect of pigmentation to spectral sensitivity) has to be checked in future work.

III. Application in laser plasma experiment

We applied imaging plate system to ultra-high intensity laser experiments on the Vulcan laser facility at Rutherford Appleton laboratory in the United Kingdom (P K Patel, 2005). Plural plates were simultaneously used as detectors for an x-ray radiography, a magnetic electron/positron spectrometer, an x-ray spectrometer with highly oriented pyrolitic graphite (HOPG) crystal. The plats are also used temporally to help alignment of a multilayer x-ray monochromatic imager, an x-ray imager with CsI phosphor coupled with CCD, and a bent crystal imager for Cu K line imaging.

HIGH ENERGY RADIOGRAPHY

High speed x-ray radiography is one of the most anticipated applications of an ultra-short pulse laser. Intense x-ray flash (~10 ps) from laser matter interaction allows observation of high velocity objects (velocity ~ 3 x 10^7 cm/sec) with minimal motion blur. Various x-ray imaging techniques has been utilized to achieve high spatial resolution with using laser plasma x-ray source (Key PRL1978, M Miyanaga1982, Landen RSI 2001, Pikuz 2001, J. A. Koch 2003, Park HS RSI2004); (1) x-ray shadowgraph with point backlight source, (2) x-ray shadowgraph with areal back lighter and x-ray imaging optics. Achievable spatial resolution of the point backlight scheme is determined by the size of the x-ray source. We applied IP system to demonstrate the performance of the point backlit imaging technique at Rutherford Appleton Laboratory. Figure 3 (a) shows the experimental setup for the radiography experiment. As an x-ray source, a samarium foil (100 x 100 x 16μm) was irradiated by Vulcan laser system at the target area west (Pulse width: 10ps, Intensity: 3x10^{18} Watt/cm^2, Wavelength: 1035nm, Pulse energy: 60 joules

on target). A gold foil with machined sinusoidal ripples (provided by General Atomics, thickness: 35um, wavelength: 20, 50, 100 μm, modulation amplitude 6 μm) was used as test object for the backlight radiography. The test object was placed 24.5 mm from the x-ray source. Shadowgraph of the object (magnification: 17) was recorded by imaging plate (FDL-UR-V) placed 416mm from the source. To minimize the apparent x-ray source size, the object was placed 90 degrees from the Sm foils surface normal. **Fig. 3 (b)** shows the backlight image recorded by IP. Perturbation of 50 μm and 100 μm ripple was resolved clearly (**Fig. 3 (c)**). The contrast of 100 μm was ~6% in peak to valley and this is smaller than ~24% contrast expected from photo-electric cross section of the gold object for 40keV emission from samarium k shell. This low contrast could be due to contribution of high energy background (>100 keV) which make less absorption through the object. The observed ~3% contrast of 20 μm ripple was even smaller than longer wavelength ripples. The wavelength of 20 μm ripple at object plane corresponds to 340 μm and the IP has good MTF ~ 0.8 in this region (~ 3 cycles per mm). There for, we believe the contrast of 20 μm ripple was mainly determined by finite width of the x-ray source.

TIME INGEGRATED X-RAY SEPCTROSCOPY

The IP was also applied to x-ray spectroscopy on ultra-intense laser experiments at Vulcan petawatt laser facility at Rutherford Appleton Laboratory. The goal of the experiment was observation of the spectral shift of cupper k-shell line emissions due to an isochoric heating of solid density plasma. The laser beam (wavelength:1035nm, pulse duration: 0.4 ~10ps) was focused on to the target with f/3 off axis parabola mirror at 28 degrees from the target normal. The focal spot diameter (6~22 μm) and laser energy (10~400J) was chosen to keep the laser

irradiation intensity I ~10^{18}-10^{19} W/cm^2. Fig. 4 (a) shows the experimental setup. To avoid the spectral shift due to Doppler broadening of expanding plasma, both side of the Cu foil was tamped by aluminum layer (~1 μm thickness). X-ray emission from 8.0~8.2 keV region was observed with using a sagittally curved highly oriented pyrolitic graphite (HOPG) crystal spectrometer. To have high throughput, spectrometer has to be set close to the target and then detector has to be operated in harsh EMP environment. A sliding stage attached to the HOPG spectrometer allows recording multiple shots without replacing IP. Fig. 4 (b) shows the raw data obtained in the experiment. Due to high dynamic range of IP, line emissions form Cu was recorded with no saturation. Fig. 4 (c) shows the x-ray spectrum from 8.0 - 8.2 keV region. With lowest energy shot (blue line, E ~11J, I = 6.6x 10^{18} W/cm^2, L =0.4mm), Kα_1 (8.048 keV) and Kα_2 (8.028 keV) lines are clearly resolved and they provided good calibration of the spectral dispersion. With higher energy shot (green line, E = 251 J, I = 3.6 x 10^{18} W/cm^2, L = 1mm), significant blue shift of Kα_1 was observed. Due to volume metric heating of the target with recalculating high energy electrons, more heating is expected with smaller target. As expected, x-ray spectrum from smaller target with almost identical laser irradiation (red line, E = 259 J, I = 3.7 x 10^{18} W/cm^2, L = 0.1 mm) showed largest blue shift.

Details of the experiment and the data analysis was completed and reported by G.Gregori (Gregori, contrib. plasma phys 45, 2005). The observed blue shift corresponds to electron temperature on the order of 200 +/- 25 eV.

IMAGING OF IMPLODED CORE

IP was applied to indirect implosion experiment at OMEGA laser facility at the University of Rochester (J. M. Sources, R. L. McCrory, C. P. verdon et al., Phys. Plasmas 3 2108(1996)). Planned cryogenic ignition experiments at the National Ignition Facility (NIF) are expected to use a fill tube to introduce liquid DT into the capsule prior to solid layer formation. This fill tube is expected to form a hydrodynamic jet during the deceleration phase of the implosion. Primal goal of this experiment is to establish diagnostic technique to experimentally evaluate the hydro-dynamic effect of fuel filling tube in indirect implosion experiment on Omega. Fig. 5 (a) shows the experimental set up. The capsules used were 510-μm-diameter, 35um thick plastic shells. The capsule was filled with 50 atm of deuterium gas fuel. In order to enhance the deformation of fuel-pusher interface close to maximum compression timing, innermost layer of the shell was doped with 1.5% of titanium as tracer. To simulate the effect of fuel filling tube, a plastic stalk (length 100μm, diameter 9 μm) was attached on capsule surface with using UV cure glue (Fig. 5 (b)). The hohlraum are 1.6 mm in diameter by 2.5 mm long with1.2mm laser entrance hole. The inner surface of the hohlraum was roughened (amplitude ~ 300 nm RMS) to mitigate imprint due to laser light specularily reflected on the hohlraum surface and focused on capsule surface. To see the ~4.8 keV x-ray emission from the titanium tracer, 3 diagnostic holes (diameter 400μm) were bored on equator of the hohlraum wall and covered with beryllium window. Since the emission from the titanium tracer is expected to be weaker than typical experiment with argon gas tracer, imaging diagnostics has to have high throughput. Observation of hydrodynamic jet requires high resolution also. To satisfy these requirement, target mounted pinhole arrays were set 4.2 mm from the capsule. The pinhole array projects multiple images on to IP located 457 mm from the object with magnification of 108. Fig. 5 (c) shows the images obtained with IP.

Generation of hydro dynamic jet was observed successfully. High magnification and large throughput of the target mounted pinhole array allowed to visualize week emission form the fuel-pusher interface.

ACKNOWLDGEMENT

We gratefully acknowledges K. Akli, W. Armstrong, H. Chen R. Clarke, R.R Freeman, R. Heathcote, D. Hey, M.H. Key, J. King, J. Kuba, K. Loughman, D. Lovas, A. McKinnon, D. Neely, P. Patel, G. Pien, V. Rekow, C. Sorce, R. Stephens, M. Takagi, J. Tellinghuisen, W. Thobald, R. Wallace, B.B. Zhang for useful discussion. N.I. appreciates W. Miller and M. Irwin of ElectroImage, Inc for the preserving collaborative efforts. This work has been performed under the auspices of U.S. Department of Energy by the University of California Lawrence Livermore National Laboratory under Contract No. W-7405-Eng-48.

Reference

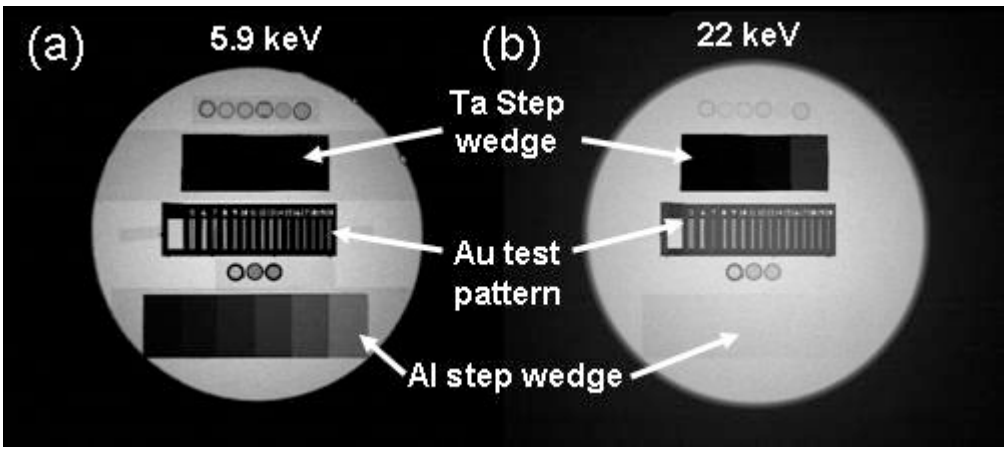

FIG. 1. Images obtained with text exposure using calibrated radioactive sources using: (a) 5.9 keV x-ray from 55Fe and (b) 22 keV x-ray from 109Cd.

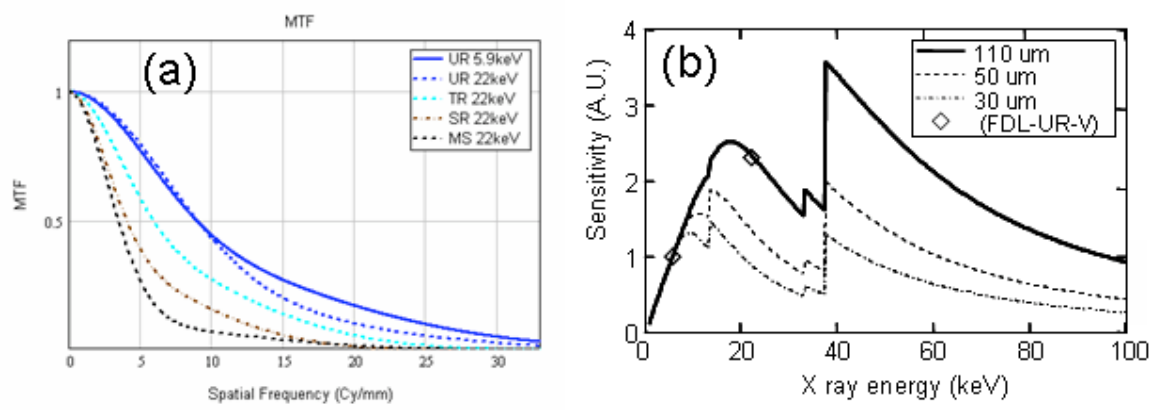

FIG. 2. Result of test exposure. (a) MTF calculated by fitting of lineout profile of the resolution test pattern image of FDL-UR-V with 5.9 keV source (blue solid line). Results of 22 keV source exposure is shown by dotted lines for: FDL-UR-V (bule line); BAS-TR (lite blue line); BAS-TR (brown line); BAS-MS (black line). (b) Spectral sensitivity calculated from photo-electric cross sections for given effective thickness of: 110 μm (solid line); 50 μm (dotted line), 30μm (dashed line). All curves are normalized by its sensitivity on 5.9 keV. Open diamond is showing the experimental result for FDL-UR-V.

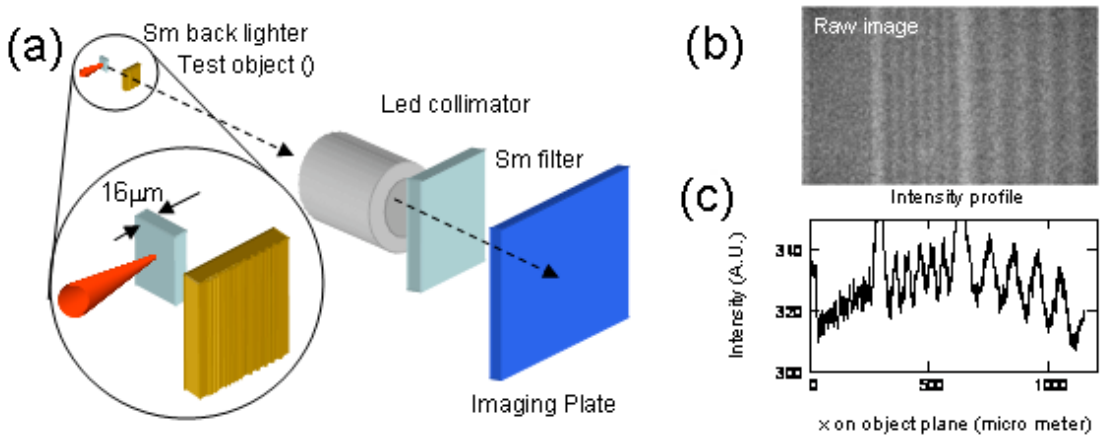

FIG. 3. (a) Experimental setup for high energy x-ray backlight experiment at Vulcan 100TW laser facility. (b) backlit image of the gold test object obtained with FDL-UR-V. (c) Lineout of the backlit image.

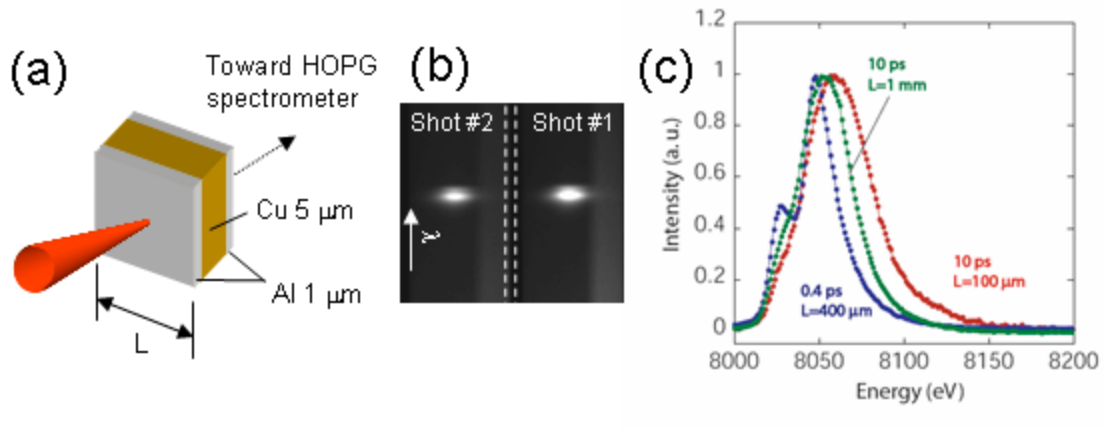

FIG. 4. (a) Experimental setup of isochoric heating experiment at Vulcan petawatt laser facility. Both surface of the cupper foil was coated by aluminum layer to surpress the effect of plasma expansion. (b) raw image obtained with IP attached HOPG crystal spectrometer. (c) Cu K line spectrum obtained: (blue line) L = 0.4 mm, laser energy 11 Joule, and laser intensity 6.6×10^{18} W/cm^2; (green line) L = 1.0mm, laser energy 251 Joule, and laser intensity 3.6×10^{18} W/cm^2 ; (red line) L = 0.1 mm, laser energy 259 Joule, and laser intensity 3.7×10^{18} W/cm^2

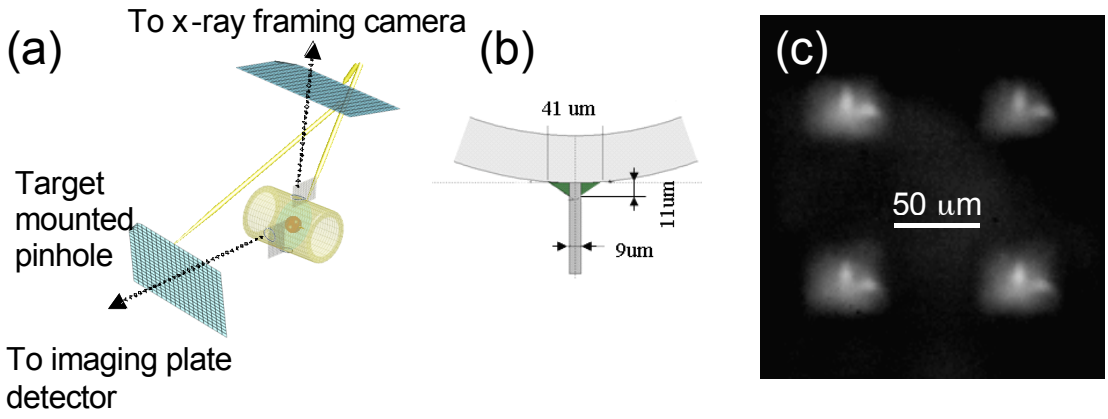

FIG. 5. (a) Experimental setup of indirect implosion experiment at Omega laser facility. (b) Plastic stalk (diameter 9 μm, length ~100 μm) was attached on the capsule surface toward laser entrance hole. (c) Self emission image of imploded core recorded by imaging plate (4 images are projected on FDL-UR-V). Vertical structure on center is jet caused by hydrodynamic effect of the stalk and glue used for attachment. Bright spot on right could be caused by unintentionally imposed bump on the initial capsule surface.